Journal of Nuclear Materials 385 (2009) 294–298

Contents lists available at ScienceDirect

Journal of Nuclear Materials

journal homepage: www.elsevier.com/locate/jnucmat

Behaviour of helium after implantation in molybdenum

C. Viaud [a,*], S. Maillard [a], G. Carlot [a], C. Valot [a], E. Gilabert [b], T. Sauvage [c], C. Peaucelle [d], N. Moncoffre [d]

[a] Commissariat à l'Energie Atomique (CEA), Cadarache, France
[b] Chimie Nucléaire Analytique & Bio-environnementale (CNAB), Gradignan, France
[c] CEMHTI-CNRS, Orléans, France
[d] Institut de Physique Nucléaire de Lyon (IPNL), Lyon, France

ARTICLE INFO

PACS:
66.30.Je
68.43.Nr
68.43.Vx

ABSTRACT

This study deals with the behaviour of helium in a molybdenum liner dedicated to the retention of fission products. More precisely this work contributes to evaluate the release of implanted helium when the gas has precipitated into nanometric bubbles close to the free surface. A simple model dedicated to calculate the helium release in such a condition is presented. The specificity of this model lays on the assumption that the gas is in equilibrium with a simple distribution of growing bubbles. This effort is encouraging since the calculated helium release fits an experimental dataset with a set of parameters in good agreement with the literature.

1. Introduction

Amongst a range of new concepts for the Generation IV, the Gas Fast Reactor is of particular interest and is designed for producing energy more efficiency and improving safety features such as a total retention of the fission products. This study deals with the behaviour of helium in molybdenum liners dedicated to the retention of these fission products. The liner will be located in the heart of the nuclear fuel element composed of alpha-emitter actinides, where the temperature will reach between 1275 and 1875 K.

The helium behaviour is a major issue for the design and durability evaluation of materials in a nuclear reactor environment. Trinkaus [1,2] has been proposed a general review of helium in metal. As insoluble gas, helium is likely to precipitate into bubbles even at very low concentration and reduce the structural integrity.

For more than 40 years works have dealt with helium behaviour in metal and especially in bcc metals, see in [2–4,12]. Particular effort was granted to describe the precipitation of helium in the bulk of the metal assisted by the supersaturation of vacancies induced by the irradiation. These studies are still at stake for the fusion reactor blanket design where refractory metals are studied under high helium doses and high energies implantations [5,6].

This paper presents the experimental characterization and modelling of the thermal behaviour of implanted helium in molybdenum. The implantation conditions (a relative low fluence (0.02 at.%) implanted at 60 keV) have been chosen so that the precipitation of the gas is expected to be in competition with its leakage at the free surface. This usual approach is a necessary first step study to the general evaluation of the behaviour of the continually implanted gas in the Gas Fast Reactor conditions. Recent results of similar studies in tungsten [7–10] present the conditions for which either the whole gas is released (0.002 at.% for 60 keV) or the gas is trapped (>0.07 at.% for 500 keV). Both extreme behaviours have been observed in molybdenum for the same conditions [11]. Here an intermediate condition (~0.02 at.% for 60 keV) is undertaken to study the helium diffusion and release in competition with a trapping process. A simple model is proposed to analyse specific experimental releases measured with a high sensitive mass spectrometer for thermal annealing sequences from 1275 to 1525 K.

The first part of this paper presents the experimental release and its specificity, obtained with a very original device, a high sensitive mass spectrometer set-up developed at the CNAB Laboratory in Bordeaux (Chimie Nucléaire Analytique & Bio-environnementale).

The second part presents briefly the assumptions made on the precipitation of the implanted helium. The last part proposes a description of a simplified model of helium release when the gas has precipitated into nanometric bubbles. Its application to the experimental release shows that the dynamic of the release strongly depends on the thermodynamic and the growth kinetics of the bubbles.

2. The experimental release and its specificity

As helium is expected to precipitate even at relatively low concentration, it is difficult to study separately the pure migration of helium atoms. Thus experimental conditions are chosen to have a balanced competition between both the precipitation and the release of implanted helium. A case is reported for which the expected release could be significant enough to be measured by a

* Corresponding author. Tel.: +33 442 25 23 86; fax: +33 442 25 32 85.
E-mail address: viaud@dircad.cea.fr (C. Viaud).

0022-3115/$ - see front matter © 2008 Published by Elsevier B.V.
doi:10.1016/j.jnucmat.2008.12.005

very high sensitive mass spectrometer and moreover the transmission electron microscopy (TEM) observations of bubbles precipitation is possible. The TEM observations are currently performed, consequently only some first results are presented in this paper to illustrate the presence of the bubble and provide some qualitative results.

A single crystal of molybdenum was ^{3}He implanted up to 1.4×10^{14} cm^{-2} (±5%) with 60 keV ^{3}He$^+$ ions. This corresponds to a maximum concentration of 0.016 at.% located at 150 nm with a 130 nm width. The sample was then annealed in a furnace connected to the high sensitive mass spectrometer set-up. Two successive isothermal annealing sequences were performed: the first one at 1275 K during 100 min where transient phenomena such as the nucleation occur; the second one at 1575 K during 180 min is the sequence of interest for the present study whose release is commented below. The cumulative releases as well as the annealing history are given in Fig. 1. The number of released gas atoms is extracted every 30 min after a volemic expansion. Prior to the measurement, the extracted gas is fractioned and purified in different volumes with getters.

After the first isothermal annealing sequence, <3% of the implanted gas has been released. In this study, this first thermal treatment is assimilated as a starting point for the following treatment where bubbles may have reach a significant size and concentration which will be provided by a TEM observation. During the second isothermal annealing sequence, the dynamic of the release starts to slow down while the cumulative value is only around 22%. The following will focus on this specificity and on the attempt to determine the origin of this slowing down dynamic.

3. Model

3.1. Assumptions on the helium precipitation

The implantation of helium atoms around 100 keV in a bcc metal mostly generates single vacancy defects [13]. During an annealing sequence, following the implantation, these supersaturated vacancies and the gas atoms tend to form bubbles. Their size distribution and concentration can be properly evaluated by solving the Fokker–Planck equations considering the thermodynamic of the system composed of a gas and defects supersaturation in the solid [14–19]. The Fokker–Planck (FP) relationships are given by Eqs. (1) and (2) with $f(x,n)$ the distribution density of the bubbles containing x helium atoms and composed of n vacancies. A numerical method for solving FP's equations has been proposed and implemented in [20,21]. This is a time expensive calculation which may not be appropriate with a long scale diffusion problem. On the other hand, Ghoniem [22] has been proposed a specific way to determine the evolution of the bubbles size by solving FP equations with the moment expansion of the size distribution. This latter method is more appropriate to any confrontation with microscopic measurements and any scale diffusion problems. However, the implementation and use of this method will be presented elsewhere

$$\begin{aligned} &\alpha = (x,n)\\ &A_\alpha = P_\alpha - Q_\alpha\\ &B_\alpha = \frac{(P_\alpha + Q_\alpha)}{2}\\ &P_\alpha \propto 4\pi \cdot D_\alpha \cdot R \cdot C_\alpha\\ &Q_\alpha = 4\pi \cdot D_\alpha \cdot R \cdot C_{\alpha,\mathrm{eq}}(R,x,n), \end{aligned} \tag{1}$$

$$\begin{aligned} &\frac{\partial f}{\partial t} = -\frac{\partial J_x}{\partial x} - \frac{\partial J_n}{\partial n}\\ &J_x = A_x \cdot f - \frac{\partial (B_x f)}{\partial x}\\ &J_n = A_n \cdot f - \frac{\partial (B_n f)}{\partial n}. \end{aligned} \tag{2}$$

As a first step, in this work we will not consider the nucleation stage and we will only consider a mean bubble size and a given concentration whose initial values can be indicated by a TEM observation. Fig. 2 shows the bubbles observed after a 1273 K at 100 min annealing sequence in a Mo single crystal implanted with He up to 2x10^{15} cm^{-2} (0.2 at.% for 60 keV). Table 1 summarizes the results of the TEM observation measured with the 0.2 at.% – implanted sample which was prepared by FIB. First this result is consistent with the assumption that helium may precipitate in the 0.016 at.% – implanted single crystal whose thermal helium release has been measured. Moreover, it indicates the expected values for the bubble size and concentration as well as the specific geometry of the problem at the end of the first annealing sequence (1273 K at 100 min).

For the evaluation of the release, the bubbles were considered reach a thermodynamic equilibrium with the gas in solution in the matrix. This equilibrium state gives the number x of helium atoms filling a bubble and the equilibrium concentration of helium in solution in the vicinity of a bubble C_{eq}. Eqs. (3) and (4) give the formalism of the latter assumptions, using the 'hard spheres' model [18,23], which is always valid, even for low and high gas densities η.

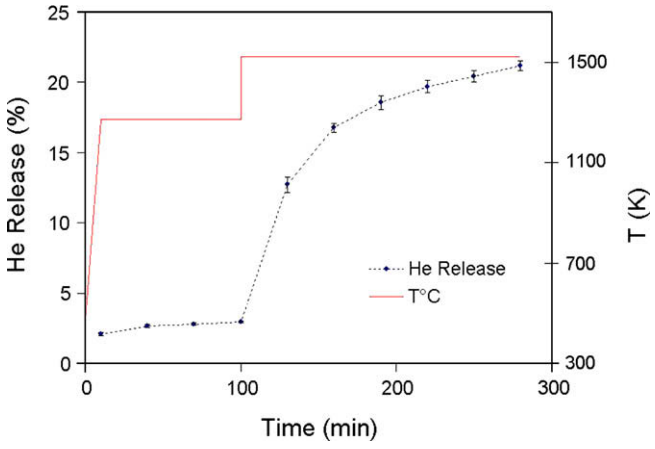

Fig. 1. Experimental helium release for two successive isothermal annealing (1275 K at 100 min and 1525 K at 180 min) for a single crystal. He implanted up to 1.4×10^{14} cm^{-2} (±5%) at 60 keV.

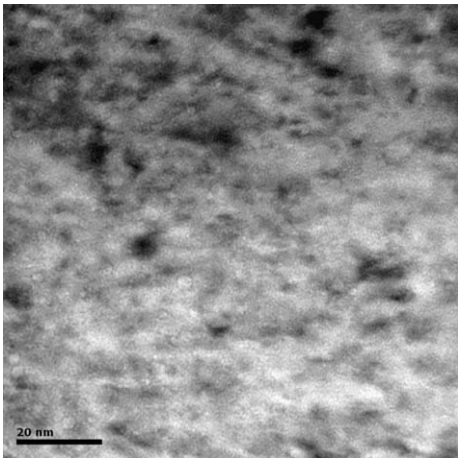

Fig. 2. TEM picture of bubbles in a Mo single crystal, He implanted with 2×10^{15} cm^{-2} (0.2 at.%) at 60 keV and annealed at 1273 K during 100 min. Note the bubbles appearing as spots in the micrograph.

Table 1
TEM conditions and measurement data.

Helium concentration (at.%)	Bubble mean radius (nm)	Bubbles concentration (cm^{-3})	Distance to the surface (nm)	Sample thickness (nm)	Annealing sequence	
					T (K)	t (min)
0.2	2	$\sim 2 \times 10^{16}$	150	80–100	1273	100

Eq. (5) gives the expression for an ideal gas obtained with η close to zero in Eqs. (3) and (4). T is the temperature; d_0, diameter of one helium atom; ψ, free enthalpy of dissolution of helium from a flat surface into the matrix; k_B, Boltzmann constant; m, mass of one helium atom; and $\hbar$, the Planck constant

$$C_{eq}(x,R) = \frac{\eta(1-\eta)^2}{\omega_0}\left(\frac{2\pi\hbar^2}{mkT}\right)^{\frac{3}{2}} e^{\left(-\frac{\psi}{kt}+\frac{PV}{xkT}+\frac{6\eta}{1-\eta}-1\right)}, \tag{3}$$

$$\eta = \frac{x\omega_0}{V}; \quad \frac{PV}{xkT} = \frac{1+2\eta^2+3\eta^3}{(1-\eta)^2}; \quad \omega_0 = \frac{\pi d_0^3}{6}, \tag{4}$$

$$C_{eq}(x,R) = x\frac{3}{4\pi R^3}\left(\frac{2\pi\hbar^2}{mkT}\right)^{\frac{3}{2}} e^{\frac{-\psi}{kT}}. \tag{5}$$

3.2. Helium steady-state diffusion in equilibrium with bubbles

3.2.1. The steady-state release of helium

A way to propose and use a simple model of helium release is to consider a steady-state regime of diffusion in which the solute gas is in equilibrium with the bubbles. The existence of the bubbles results to an advanced state in the precipitation that can be provided by a first annealing sequence as already mentioned. In this case, the nucleation of bubbles and the resulting transient gas release is not under consideration. Fig. 3 illustrates the configuration of the steady-state gas diffusion assumed in the proposed model, with C_{He} the concentration of helium in solution.

For this configuration the rate equation are written in Eq. (6) for $C_{He}(t)$ and $x(t)$ in a volume $L \cdot l^2$ with L, the distance between the bubbles and the free surface; l, the distance between two bubbles. Note that, l is in relation with the concentration of bubbles C_b ($C_b = l^{-3}$). D_0 is the diffusion coefficient of helium in the metal. The first term in the right hand side is an approximation of the leakage flux valid for steady-state diffusion. The second term corresponds to the sink/emission term of one bubble assuming the diffusion-controlled solution of the steady-state diffusion problem for an isolated spherical bubble [24]

$$\begin{cases} Ll^2\,\dot{C}_{He}(t) = -\frac{D_0}{L}C_{He}(t)l^2 - 4\pi R D_0(C_{He}(t) - C_{eq}(x,R)) \\ \dot{x}(t) = 4\pi R D_0(C_{He}(t) - C_{eq}(x,R)), \end{cases} \tag{6}$$

which leads to

$$\begin{cases} C_{He}(t) = -(v_1+v_2)C_{He}(t) + v_2 C_{eq}(x,R) \\ x(t) = v_2 Ll^2(C_{He}(t) - C_{eq}(x,R)) \end{cases}$$
$$v_1 = \frac{D_0}{L^2} \tag{7}$$
$$v_2 = \frac{4\pi R D_0}{Ll^2}$$

In Eq. (7), one assumes that C_{He} reaches a stationary state prior to any variation of x which gives

$$C_{He}(t) = \frac{v_2}{v_1+v_2}C_{eq}(x(t),R). \tag{8}$$

Hence one derives by substituting Eq. (8) in Eq. (7)

$$\dot{x}(t) = -\frac{v_2 v_1}{v_1+v_2}Ll^2 C_{eq}(x(t),R). \tag{9}$$

Now one can evaluate the number of released helium atoms $N(t)$

$$N(t) = \int_0^t \frac{D_0}{L}l^2 C_{He}(t)dt. \tag{10}$$

Eqs. (9) and (10) gives the gas fraction release $r(t)$ with N_0 the initial number of helium atoms in a bubble

$$r(t) = \frac{1}{N_0}\int_t^0 \frac{v_2 v_1}{v_1+v_2}Ll^2 C_{eq}(x,R)dt = \frac{1}{N_0}\int_{x(t)}^{x_0=N_0} dx = 1 - \frac{x(t)}{N_0}. \tag{11}$$

For an ideal gas, according to Eq. (5)

$$C_{eq}(x,R) = \gamma(R)x. \tag{12}$$

Then, if v_1 and v_2 are kept constant, the gas fraction release $r(t)$ becomes

$$\begin{aligned} r(t) &= 1 - e^{-t/\tau} \\ \text{with } \tau &= \tfrac{v_1+v_2}{v_1 v_2}\tfrac{1}{l^2 L\gamma} = \tfrac{1}{l^2 L\gamma}(\tau_1+\tau_2), \end{aligned} \tag{13}$$

τ_1 and τ_2 are the characteristic times of the diffusion mechanism and the trapping process respectively. The solution in Eq. (13), with a pure asymptotic exponential shape, estimates the gas release to saturate around 100%. It will be seen in the experimental part that the gas release saturates well below 100%. This result is illustrated in Fig. 4 in Section 3.3.

3.2.2. A steady-state diffusion coupled with the evolution/growth of the bubbles

Up to here, any evolution of the bubbles during the thermal annealing sequence has been considered. In this subsection we present the major control that the bubble growth can have on the gas release dynamic.

As previously given configuration of bubbles with a radius $R(t)$ in equilibrium with the helium in solution is considered. From Eq. (2), one can derive an approximated form of the growth kinetics of a bubble in function of the vacancy concentration C_v (in fraction of site)

$$\dot{V} = 4\pi R^2 \dot{R} = 4\pi R D_v \Omega(C_v(t) - C_{v,eq}(x,R)), \tag{14}$$

with D_v the diffusion coefficient of vacancies and according to [18,23]

$$C_{v,eq}(x,R) = e^{\frac{1}{kT}\left(-\varphi+\frac{2\sigma\Omega}{R}-P\Omega\right)} = C_{v0}e^{\frac{2\sigma\Omega}{RkT}-\frac{P\Omega}{kT}}, \tag{15}$$

with φ, the free energy of dissolution of vacancy from a flat surface into the matrix; σ, the surface tension; and Ω, the atomic volume of the matrix.

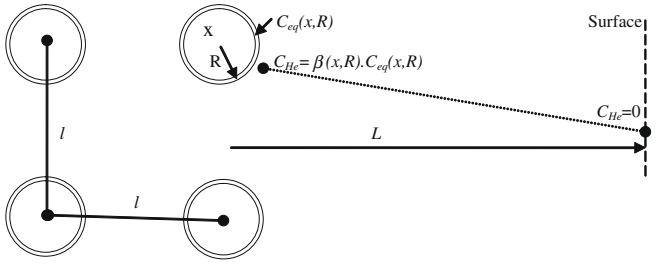

Fig. 3. Illustration of the configuration of the bubbles and the gas in solution during the steady-state regime considered in the model.

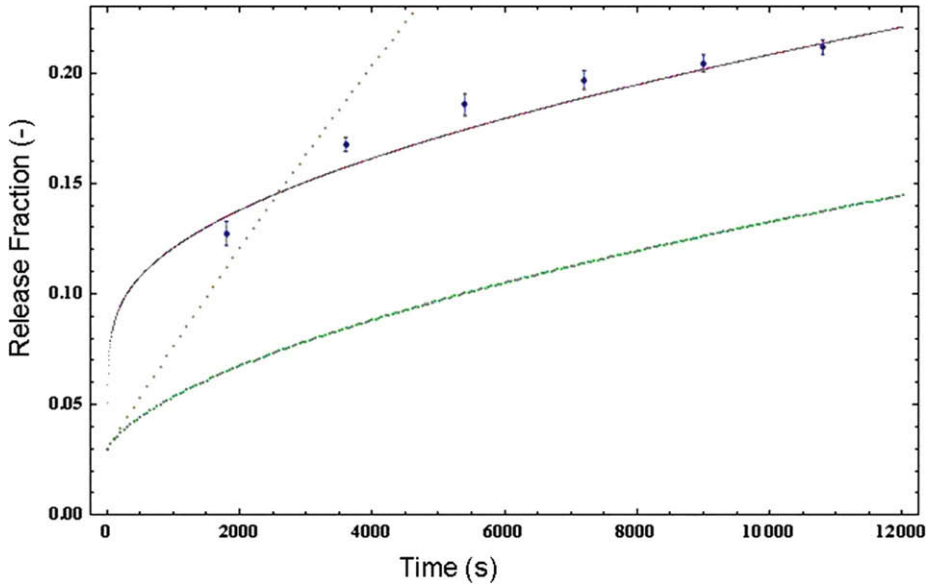

Fig. 4. Cumulative helium release during the second isothermal annealing sequence: dots->experimental data; line->calculation with the bubble growth and the hard sphere model gas; dash line-> calculation with no bubble growth and the ideal gas state equation; discontinuous line-> calculation with the bubble growth for an ideal gas. For the numerical values of the parameters see Table 2.

Assuming $C_v = C_{v0}$, the thermal concentration of vacancies, and expanding e^x at 0, one obtains

$$\dot{R} = \frac{D_v \Omega C_{v0}}{kTR}\left(P - \frac{2\sigma}{R}\right). \tag{16}$$

For an ideal gas it becomes

$$\dot{R} = \frac{3D_v\Omega C_{v0}}{4\pi R^4} x\left(1 - \frac{R^2}{R_c^2 x}\right) \quad \text{with } R_c = \sqrt{\frac{kT}{8\pi\sigma}}. \tag{17}$$

Consequently a bubble will tend intrinsically to have a radius equal to $\sqrt{xR_c}$ and accommodate the decrease of x due to the loss of helium gas. For simplicity, we still assume that the distance l between two bubbles (i.e., the bubble concentration) remains constant as well as L.

For an ideal gas, Eq. (9) can be rewritten substituting C_{eq} by $x \cdot V_m/R^3$ (equivalent to Eq. (12))

$$\dot{x}(t) = -\frac{v_1 v_2(R)}{v_1 + v_2(R)} Ll^2 V_m \frac{x}{R(t)^3}. \tag{18}$$

As v_2 is proportional to $R(t)$, in Eq. (18) we note that the increase of $R(t)$ is likely to induce the slowing down of the helium release which is observed in the experiment. This effect is notable if the response times of both $x(t)$ and $R(t)$ are in the same order of magnitude.

Finally the system to be solved is for a non ideal gas (hard sphere model)

$$\dot{x}(t) = -\frac{v_1 v_2(R)}{v_1 + v_2(R)} Ll^2 C_{eq}(x(t), R) \tag{19}$$

$$\dot{R} = \frac{D_v \Omega C_{v0}}{kTR}\left(P(x,R) - \frac{2\sigma}{R}\right). \tag{20}$$

3.3. An application of the model to experimental measurements of helium release

The model enables to simulate the experimental release of the second annealing sequence by solving the system of Eqs. (19), (20), and (11). The first annealing sequence can provide an order of magnitude of the two parameters l and L. Indeed to be consistent with the value of the 'first release' (3%), l, L and R_0 (the bubble radius at the beginning of the second annealing sequence) are in relation: the sink strength of the free surface v_1 must be in the same order of magnitude as the sink strength of the bubbles v_2. Moreover, the fraction of implanted gas closer to the surface than L has to be less than 6% (twice the first release since one half reaches the surface when the other is trapped in the bubbles). Consequently, considering a bubble radius R_0 starting from some nanometers and the helium depth profile given by a TRIM calculation, one derives $l \cong L = 70$ nm. This value is consistent with the concentration of the bubbles derived from the TEM observation of the He 0.2 at.% – implanted sample. Indeed a concentration of $2\text{x}10^{15}$ cm^{-3} (extrapolated from the TEM results) corresponds to a distance of 70 nm between each bubble.

The results for three different calculations are plotted in Fig. 4, which are compared to the experimental data. One is the result for an ideal gas release in equilibrium with non growing bubbles. Another is the result for an ideal gas release in equilibrium with growing bubbles and the last one is the release for a non ideal gas in equilibrium with growing bubbles. First this comparison shows the necessity to propose a model with a 'slow down' dynamic then it present the encouraging fit that the general form of the model can provide especially with the 'hard sphere' equation of state. Table 2 summarizes the input parameters, among which some are compared with the literature. From this result, the order of magnitude of the diffusion coefficient of helium can be derived as well as the free enthalpies of dissolution of helium from a flat surface into the matrix, respectively D_0, ψ can be derived (this result is only qualitative for the moment so no relevant error values under 50% can be provided here). Their values are consistent with previous published results: recently [25] found an interstitial migration energy around 0.06 eV for helium in steel (another bcc metal whose migration mechanisms are expected to be similar to Mo); Van Veen [26,27] and Casper [28] determined experimentally the enthalpy ψ for W and Mo around 3.2 and 4.0 eV, respectively. One can conclude that this consistency with the literature is satisfying and strengthens the validity of the proposed assumptions.

Fig. 5 shows the calculated evolution of the bubble radius. This result as well as the bubbles concentration ($l = 70$ nm) considered in the calculation will be compared to coming TEM observations.

Table 2
parameters used in the calculations. The values in bold were fixed.

$E_{m,He}$ (eV)	$E_{m,v}$ (eV)	ψ (eV)	φ (eV)	l (nm)	L (nm)	R_0 (nm)	N_0	σ (erg · cm^{-2})	d_0 (pm)	Ω (cm^3)
Values for both ideal and non ideal gas										
0.09	1.35	3.83	3.05	70	70	1.8	6860	500	130	1.5×10^{-23}
Values for an ideal gas without the bubble growth										
0.09	1.35	3.83	3.05	70	70	2.0	6860			
Comparison with the literature and sources										
0.06[25]*	1.3 [27]	3.2 [28]	3 [29]							

* In Fe.

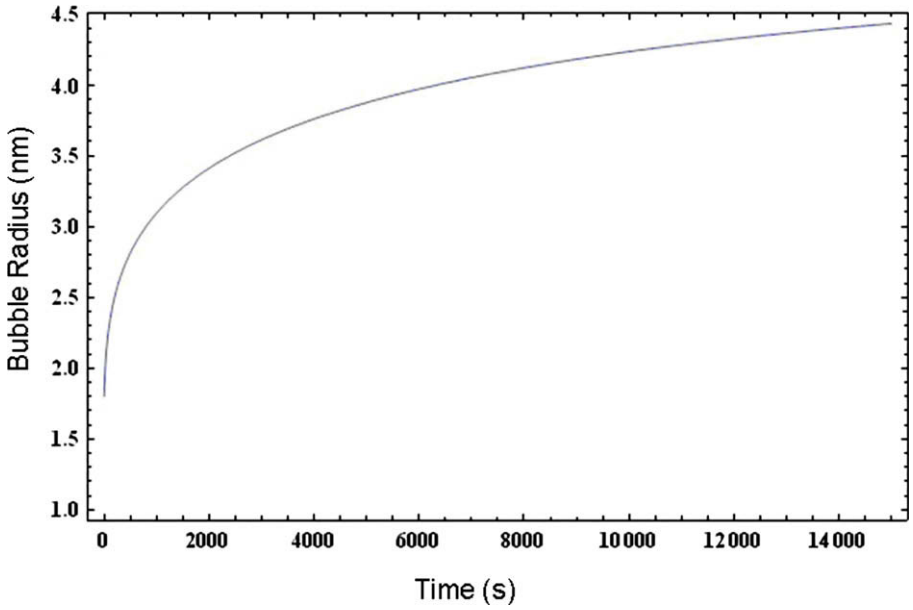

Fig. 5. Bubble radius evolution as calculated with the 'hard sphere model' and the growth of the bubbles (for the numerical values see Table 2).

Note that both $R(t)$ and l are consistent with the upper values indicated by the TEM observation presented above.

4. Conclusion

This work intends to contribute to the study of the release of implanted helium when the gas has already precipitated into nanometric bubbles close to the free surface. This issue is relevant for the study of nuclear materials in an alpha-emitting environment. A specific simplified model has been developed which is able to simulate 'a slowing down' helium release when the gas is in equilibrium with a simple distribution of growing bubbles. This first attempt is encouraging since it fits an experimental dataset with a set of parameters in good agreement with the literature. More experimental releases and TEM observations will be confronted to this model to confirm its validity. Finally as a next step, the early stage of nucleation and more complicated evolution of bubbles (such as their ripening) could be integrated. This would provide more confident results and enable to simulate more accurately transient releases of any annealing sequence.

References

[1] H. Trinkaus, Radiat. Eff. 78 (1983) 189.
[2] H. Trinkaus, B.N. Singh, J. Nucl. Mater. 323 (2003) 229.
[3] W.D. Wilson, Sandia Laboratories Report, SAND75-8740, 1975.
[4] H. Wiedersich, J.L. Katz, J. Nucl. Mater. 51 (1974) 287.
[5] H. Iwakiri, J. Nucl. Mater. 283–287 (2000) 1134.
[6] K. Morishita, J. Nucl. Mater. 353 (2006) 52.
[7] Fu Zhang, J. Nucl. Mater. 329–333 (2004) 692.
[8] N. Hashimoto, J. Nucl. Mater. 347 (2005) 307.
[9] S.B. Gilliam, J. Nucl. Mater. 347 (2005) 289.
[10] A. Debelle, J. Nucl. Mater. 362 (2007) 181.
[11] C. Viaud, G. Carlot, Thesis Lyon 1, Physics and Astrophysicsin, 2008.
[12] C.J. Ortiz, J. Caturla, C.C. Fu, F. Willaime, Phys. Rev. B 75 (2007) 100102(R).
[13] R.E. Stoller, G.R. Odette, B.D. Wirth, J. Nucl. Mater. 251 (1997) 49.
[14] S. Sharafat, N.M. Ghoniem, J. Nucl. Mater. 122&123 (1984) 531.
[15] N.M. Ghoniem, S. Sharafat, J. Nucl. Mater. 117–123 (1983) 96.
[16] H. Trinkaus, Phys. Rev. B 27 (1983) 12.
[17] L.K. Mansur, W.A. Coghlan, J. Nucl. Mater. 119 (1983) 1.
[18] A.E. Volkov, A.I. Ryazanov, J. Nucl. Mater. 273 (1999) 155.
[19] R.E. Voskoboinikov, A.E. Volkov, J. Nucl. Mater. 282 (2000) 66.
[20] S. Sharafat, Thesis, UCLA-ENG-8604, PPG-930, 1986.
[21] A. Barbu, CEA report SRMP/DTM/DEN/CEA, 2007.
[22] N.M. Ghoniem, Phys. Rev. B 39 (1988) 16.
[23] R. Balescu, Equilibrium and Nonequilibrium Statistical Mechanics, Wiley, New York, 1975.
[24] A.E. Volkov, Metallofizika 10 (1988) 63.
[25] C.C. Fu, F. Willaime, Phys. Rev. B 72 (2005) 064117.
[26] A.V. Federov, A. van Veen, Comput. Mater. Sci. 9 (1998) 309.
[27] C. Roodebergen, A. van Veen, L.M. Caspers, Chemistry and Physics, Chemical and Physical Engineering 1 (1975) 107.
[28] L.M. Caspers, A. van Veen, A.A. van Gorkum, Phys. State Sol. (a) 37 (1976) 371.
[29] T.R. Mattsson, A.E. Mattsson, Phys. Rev. B 66 (2002) 214110.